

Methane Activation by Naked Rh⁺ Atoms. A Theoretical Study

Joakim Westerberg and Margareta R. A. Blomberg*

Department of Physics, Stockholm University, S-113 85 Stockholm, Sweden

Received: February 25, 1998; In Final Form: June 24, 1998

The potential energy surface of the endothermic reaction $\text{Rh}^+ + \text{CH}_4 \rightarrow \text{RhCH}_2^+ + \text{H}_2$ is calculated using high-accuracy quantum chemical methods. The results agree with recent results from ion beam mass spectrometry, indicating that there is no barrier in excess of the endothermicity of the H_2 elimination reaction. All structures on the potential surface are optimized at the density functional theory level, using the empirically parametrized hybrid functional B3LYP. Relative energies are calculated both at the B3LYP level, using large basis sets, and at the parametrized configuration interaction (PCI-80 (MCPF)) level.

1. Introduction

Methane activation by transition metal centers is an important step in the transformation of the inert methane molecule to more useful products. C–H activation in saturated hydrocarbons was first observed to occur for transition metal complexes some 15 years ago.^{1–5} To obtain a more detailed picture of the reaction mechanism, a large number of experiments have been performed on the gas-phase reaction between methane and naked metal cations, see, for example, refs 6–8. Also many theoretical studies have been performed on the reaction of methane and naked metal cations, see, for example, refs 9–12.

In the present study the endothermic reaction



is investigated. There have been several experimental studies performed on the Rh⁺ plus methane system.^{13–17} Byrd and Freiser reported in 1982¹³ that Rh⁺ does not react with methane at thermal energies. This was confirmed by Beauchamp et al. in 1986.¹⁴ The reverse reaction was investigated by Jacobson and Freiser in 1985.¹⁵ They found that RhCH₂⁺ reacts easily with H₂ at thermal energies to form Rh⁺ + CH₄. In 1993, Musaev et al. presented theoretical results for the RhCH₂⁺ + H₂ reaction,¹⁸ based on MR-SDCI-CASSCF calculations, which were partly in contradiction to the experimental results. The reaction $\text{RhCH}_2^+ + \text{H}_2 \rightarrow \text{Rh}^+ + \text{CH}_4$ was indeed calculated to be exothermic, in agreement with the experimental results. However, they obtained an H–H activation barrier of about 10 kcal/mol,¹⁸ in contradiction to the fast reaction of RhCH₂⁺ with H₂ in the gas phase. A few years later, in 1995, Armentrout and Chen¹⁶ used guided ion beam mass spectrometry to study the reaction of Rh⁺ and CH₄ in detail. Their results definitely show that for the H₂ elimination reaction there is no barrier in excess of the endothermicity, which is thus in disagreement with the theoretical results in ref 18. In the present study the B3LYP and PCI-80 methods are used to investigate the potential energy surface for the Rh⁺ + CH₄ reaction. The purpose with this study is 2-fold. The first goal is to describe in detail the mechanism for the activation of methane by Rh⁺. The second goal is to assess the accuracy of the theoretical methods used, by the comparison to accurate experimental information on the same processes.

2. Computational Details

The calculations were performed in two steps. First, all stationary points of interest were localized at the B3LYP level, a density functional theory (DFT) type of calculation based on hybrid functionals, and with the use of double- ζ basis sets. In a second step the energy was evaluated for the optimized geometries using large basis sets with polarization functions. The final energy evaluation was performed both at the B3LYP level^{19–22} and at the PCI-80 (parametrized configuration interaction with parameter 80) level.^{23,24}

The ab initio calculations were performed using the modified coupled pair functional (MCPF) method,²⁵ which is a size-consistent, single reference state method. The zeroth order wave function was determined at the Hartree–Fock level. If standard double- ζ plus polarization (DZP) basis sets are used, it has been shown that about 80% of the correlation effects on bond strengths are obtained irrespective of the system studied. A good estimate of a bond strength is obtained by simply adding the missing 20% of the correlation effects, and this is what is done in the PCI-80 scheme.²³ The parameter 80 is thus an empirical parameter chosen to give agreement with experiment for a standard benchmark test²⁴ consisting of 32 first-row molecules used in reference ref 26. The present ab initio calculations were performed using the STOCKHOLM set of programs.²⁷

In the B3LYP calculations a relativistic ECP (Hay and Wadt,²⁸) was used for the rhodium atom. In the geometry optimizations, the 4s and 4p core orbitals are described by a single- ζ contraction while the valence 4d, 5s, and 5p orbitals are described by a double- ζ basis and the outermost 4d basis function is diffuse. The rest of the atoms are described by a standard double- ζ basis sets. At the same level force-constant matrices were calculated in all optimized stationary points, and the zero-point vibrational corrections are added to all relative energies. Thermal corrections are expected to be very small and are therefore not considered. In one single case, the singlet state of the Rh(CH₄)⁺ molecular complex, the B3LYP method could not be used in the geometry optimization. For that case, the methane geometry was frozen from the corresponding triplet state and the Rh–C distance was optimized pointwise at the PCI-80 level. The final B3LYP energy calculations were performed using the large 6-311+G(2d,2p) basis set for hydrogen, carbon, and oxygen. This basis set has two polariza-

TABLE 1: Relative Energies in kcal/mol

	Becke3LYP	PCI-80	exptl
$\text{Rh}^+ + \text{CH}_4 \rightarrow \text{RhCH}_2^+ + \text{H}_2$			
Singlet			
$\text{Rh}^+ + \text{CH}_4$		31.8	
$\text{Rh}(\text{CH}_4)^+$		8.0	
TS	17.4	13.7	
$\text{RhH}(\text{CH}_3)^+$	14.3	6.5	
TS	17.4	9.7	
$\text{Rh}(\text{CH}_2)(\text{H})_2^+$	7.8	1.4	
TS	9.0	1.9	
$\text{Rh}(\text{CH}_2)(\text{H}_2)^+$	9.0	1.2	
$\text{RhCH}_2^+ + \text{H}_2$	28.0	20.5	22.6
Triplet			
$\text{Rh}^+ + \text{CH}_4$	0.0	0.0	0.0
$\text{Rh}(\text{CH}_4)^+$	-11.5	-14.2	
TS	7.8	8.8	
$\text{RhH}(\text{CH}_3)^+$	7.8	8.5	
TS	46.2	48.9	
$\text{Rh}(\text{CH}_2)(\text{H}_2)^+$	23.5	28.5	
$\text{RhCH}_2^+ + \text{H}_2$	32.4	37.3	
$\text{RhH}^+ + \text{CH}_3$			
$\text{Rh}^+ + \text{CH}_4 \rightarrow \text{RhH}^+ + \text{CH}_3$	58.1	55.9	65.0
$\text{Rh}^+ + \text{CH}_4 \rightarrow \text{RhCH}_3^+ + \text{H}$			
$\text{RhCH}_3^+ + \text{H}$	66.1	57.6	69.4

tion functions on all atoms and also diffuse functions. For rhodium, the valence basis set used for the geometry optimizations was expanded by uncontracting one s, one p, and one d function, and by adding one more d function (even tempered) and two f functions contracted from three primitive f functions. The PCI-80 energy calculations were performed using a modified Huzinaga all electron basis set for rhodium,²⁹ yielding a (17s,13p,9d,3f) primitive basis, contracted to [7s,6p,4d,1f]. The core orbitals are all totally contracted, except for 4s and 4p. The 4s, 4p, 5s, and 5p orbitals are described by a double- ζ basis set, and the 4d orbital by a triple- ζ contraction. For carbon the primitive (9s,5p) basis of Huzinaga was used, contracted according to the general contraction scheme to [3s,2p], and one d function was added. For hydrogen the primitive (5s) basis from Huzinaga was used augmented with one p function and contracted to [3s,1p]. The energies are calculated relative to the atomic state of the metal ion that is considered to be most important in forming the chemical bonds ($^5\text{F}(4d^7 5s^1)$), and the correction to the ^3F ground state is obtained using the experimental splitting. This procedure has previously been found to give accurate results, partly canceling errors in calculated atomic spectra.³⁰

3. Results

The calculated relative energies at both the PCI-80 and B3LYP levels for all stationary points are given in Table 1, and the corresponding potential energy surfaces are shown in Figure 1.

The Rh^+ cation has a ^3F ground state, and the initial steps of the reaction with methane occur on a triplet potential surface. A spin crossing occurs in the region of the $\text{RhH}(\text{CH}_3)^+$ insertion product, and the singlet state becomes lowest in energy. There is no further spin crossing on the H_2 elimination surface, and the end RhCH_2^+ product has a singlet ground state. Following the lowest points on the potential energy surface, there is no potential barrier in excess of the endothermicity for the H_2 elimination reaction. This result is in agreement with experiment.¹⁶ The $\text{Rh}^+ + \text{CH}_4 \rightarrow \text{RhCH}_2^+ + \text{H}_2$ reaction path has previously been studied theoretically by Musaev et al.,¹⁸ using

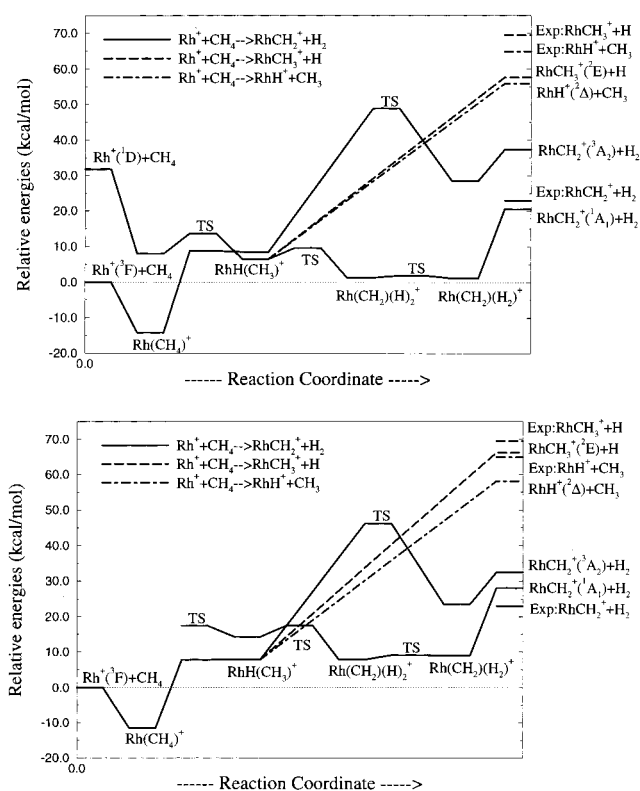


Figure 1. (a, top) The potential energy surface for the reaction $\text{Rh}^+ + \text{CH}_4 \rightarrow \text{RhCH}_2^+ + \text{H}_2$ using PCI-80. (b, bottom) The potential energy surface for the reaction $\text{Rh}^+ + \text{CH}_4 \rightarrow \text{RhCH}_2^+ + \text{H}_2$ using Becke3LYP and the large basis set.

MR-SDCI-CASSCF calculations with double- ζ plus polarization basis set. The initial CH-insertion step of the reaction has been studied theoretically by Blomberg et al., using the single reference MCPDF method with a double- ζ plus polarization basis set.¹⁰ Below we will discuss the different steps in the reaction and make comparisons to experiment and previous calculations.

The first step on the reaction path is the formation of an electrostatically bound complex, $\text{Rh}(\text{CH}_4)^+$ (Figure 2a). The triplet state of the molecular complex lies 14.2 kcal/mol below the reactants at the PCI-80 level and 11.5 kcal/mol at the B3LYP level. These results agree well with the results in ref 10, 13.0 kcal/mol, and the results in ref 18, 6.4–16.8 kcal/mol, depending on the method used. The molecular complex was found to have a tilted η^3 coordination with C_s -symmetry (see Figure 2a), 0.9 kcal/mol lower than the η^2 coordination. A frequency calculation on the η^2 structure results in two imaginary frequencies, with eigenvectors clearly indicating symmetry breaking to the tilted η^3 coordination. In ref 10 the η^2 coordination (C_{2v} symmetry) was found to be 3.4 kcal/mol lower than η^1 (C_{3v} symmetry), and also in ref 18 η^2 coordination was found to be the ground-state structure. The coordinated hydrogen closest to Rh has an optimized C–H distance of 1.13 Å (Figure 2a), as compared to 1.10 in free CH_4 , indicating an agostic interaction. The Rh–C distance obtained is 2.54 Å, which can be compared to 2.65 Å in ref 10 and 2.83 Å in ref 18. The singlet state of the $\text{Rh}(\text{CH}_4)^+$ complex was found to have a Rh–C distance of 2.49 Å. The energy for the singlet lies 23.8 kcal/mol below $\text{Rh}^+(^1A_1) + \text{CH}_4$ at the PCI-80 level. The low-spin (singlet) state of Rh^+ thus forms a more bound complex than the high-spin (triplet) state, in agreement with previous results^{10,31,32} for other transition metal complexes. In the B3LYP calculations on the excited singlet state, the ground-state triplet was mixing in for both the Rh^+ atom and the $\text{Rh}(\text{CH}_4)^+$

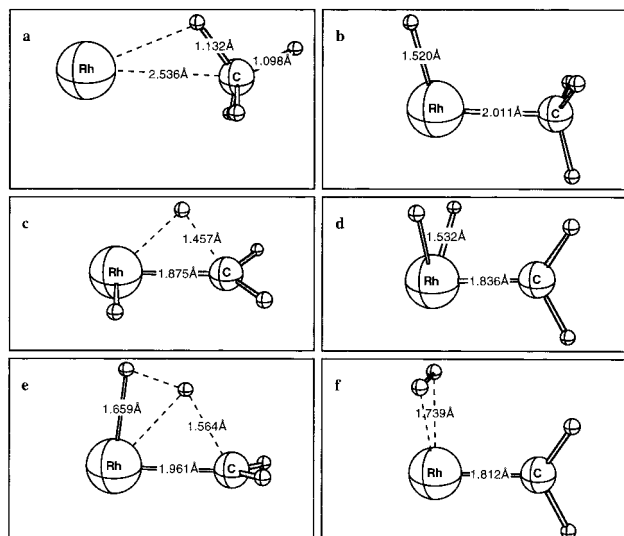


Figure 2. (a) Structure for the molecular complex $\text{Rh}(\text{CH}_4)^+$. (b) CH insertion product $\text{RhH}(\text{CH}_3)^+$ (singlet). (c) Transition state leading to the carbene dihydride (singlet). (d) Carbene dihydride $\text{HRhH}(\text{CH}_2)^+$ (singlet). (e) Four-center transition state leading directly to the H_2 molecular complex (triplet). (f) Molecular complex $(\text{H}_2)\text{Rh}(\text{CH}_2)^+$ (singlet).

molecular complex, and those results have therefore been excluded.

The next step in the reaction is the cleaving of the C–H bond (oxidative addition), resulting in the insertion product, Figure 2b. Insertion products were localized for both the triplet and the singlet states and were found to have C_s symmetry, with the two hydrogens defining the symmetry plane together with the metal, trans to each other with respect to the Rh–C bond. In ref 18 these hydrogens were found to be cis to each other. For the triplet state, the energy for the insertion product increases considerably compared to the electrostatic complex, by 22.7 kcal/mol (PCI-80) or 19.3 kcal/mol (B3LYP). For the singlet state, on the other hand, the insertion product and the molecular complex are more similar in energy. At the PCI-80 level the insertion product is 1.5 kcal/mol below the electrostatic complex. This difference between the singlet and triplet states in the stability of different structures leads to a spin crossing in this region of the potential surfaces (see further below). The triplet transition state optimized with the double- ζ basis set actually disappears when the larger basis set is used in the single-point energy calculations (B3LYP). At the PCI-80 level the energy for the transition state is very close to the insertion product, only 0.3 kcal/mol higher. The geometry obtained for the transition state is also very close to the insertion product. These results are in agreement with the results in reference ref 18 and 10, where no true minimum was found for the insertion product on the triplet surface. On the singlet surface, on the other hand, there is a minimum for the insertion product with an elimination barrier of 7.2 kcal/mol at the PCI-80 level and 3.1 kcal/mol at the B3LYP level. As mentioned above there is a spin crossing occurring in this region, making the singlet state lowest for the later parts of the reaction path. According to PCI-80, in the region of the insertion product the energy for the singlet state is 2.0 kcal/mol lower than the triplet state, while at the C–H insertion transition state the singlet state is higher by 4.9 kcal/mol. B3LYP, on the other hand, gives the triplet state lower than the singlet state for both the transition state, by 9.6 kcal/mol, and the insertion product, by 6.5 kcal/mol, indicating that the spin crossing occurs after the insertion product region. In ref 18, the insertion product is found to have a triplet ground

state by 13.0 kcal/mol. Perry³³ finds the triplet state to lie 1.4 kcal/mol below the singlet state. The Rh–C distance of 2.01 Å obtained for the singlet insertion product can be compared to 2.06 Å in ref 18. The H–Rh–C angle was found to be 108.6°, compared to 113.3° in ref 18.

On the singlet surface, the next step in the reaction chain is a migration of a second hydrogen from carbon to the metal, leading to a carbene dihydride (see Figure 2c,d). This α -elimination has an activation energy of 3.1 kcal/mol at the PCI-80 level and 3.2 kcal/mol at the B3LYP level. The dihydride lies 5.1 kcal/mol below the singlet insertion product according to PCI-80 and 6.5 kcal/mol below according to B3LYP. The Rh–C bond distance was found to be as short as 1.84 Å, which is an indication of a Rh–C double bond. According to the Mulliken population analysis, there is some 5s character (0.47) on the metal. The metal still has close to eight 4d electrons and thus does not have a full +1 charge. The charge distribution given by the Mulliken population analysis indicates a small charge transfer from the metal to the hydrogens, leaving a charge of +0.32 on the metal, which can be compared to +0.58 for the insertion product. The electronic structure of the metal can be seen as a mixing of the excited $4d^75s$ state of Rh^+ , having two unpaired electrons to form a double bond with C, besides the two hydride bonds, and the neutral Rh ($4d^85s$) forming a single covalent bond with C. In the next step the two hydrogens rearrange easily to form an H_2 molecule electrostatically bound to the metal (Figure 2f). The activation energy is 0.5 kcal/mol at the PCI-80 level and 1.2 kcal/mol at the B3LYP level. This reductive elimination step is exothermic by 0.2 kcal/mol according to PCI-80 and endothermic by 1.2 kcal/mol according to B3LYP. In the last step H_2 can be eliminated in an endothermic reaction, by 19.3 kcal/mol at the PCI-80 level and by 19.0 kcal/mol at the B3LYP level. This last step leaves RhCH_2^+ in its ground singlet state.

For the reaction step described in the previous paragraph an important difference between the present study and the one in ref 18 occurs. In ref 18, no dihydride was found for the singlet state. Therefore, the transition state for the α -elimination on the singlet surface found in ref 18 is a high-lying four-center transition state, similar to the one found for the triplet state discussed below and shown in Figure 2e. Such a transition state leads directly to RhCH_2^+ with H_2 electrostatically bound. The four-center transition state for the α -elimination on the singlet surface results in a barrier in excess of the endothermicity, by 11.3 kcal/mol,¹⁸ in contradiction to the experimental results indicating no barrier in excess of the endothermicity for the methane activation reaction by Rh^+ .¹⁶

Following the potential surface for the triplet state instead it can be seen in Figure 1 that the energy increases considerably after the first C–H insertion product. In the triplet state the rhodium cation cannot at the same time form two covalent bonds to the carbene and another two covalent bonds to the hydrides. A doubly bound carbene with the H_2 molecule electrostatically bound was found to be the energetically most favorable structure, 20.0 kcal/mol above the C–H insertion product at the PCI-80 level and 15.7 kcal/mol above at the B3LYP level. To reach this structure from the insertion product, a four-center transition state is passed, see Figure 2e, 40.4 or 38.4 kcal/mol above the insertion product at the PCI-80 and B3LYP levels, respectively. In the last endothermic reaction step, by 8.8 kcal/mol (PCI-80) or 8.9 kcal/mol (B3LYP), H_2 is eliminated yielding RhCH_2^+ in the excited triplet state.

Starting with the triplet ground state of $\text{Rh}^+ + \text{CH}_4$ and going to the singlet ground state of the $\text{RhCH}_2^+ + \text{H}_2$ end product,

the overall reaction is endothermic by 20.5 kcal/mol (PCI-80) or 28.0 kcal/mol (B3LYP) with no barrier in excess of this. Both these results are in reasonably good agreement with the experimental¹⁶ endothermicity of 22.6 kcal/mol. The Rh–C bond energies in the singlet ground state of RhCH_2^+ derived from these reaction energies are 87.0 kcal/mol (PCI-80), 79.3 kcal/mol (B3LYP), and 85.1 kcal/mol (experiment). Thus, this bond energy is in very good agreement with experiment for PCI-80, and at the B3LYP level the agreement with experiment is reasonably good. The triplet excited state of RhCH_2^+ is calculated to lie 16.8 kcal/mol above the ground-state singlet at the PCI-80 level and only 4.4 kcal/mol up at the B3LYP level. This large difference between PCI-80 and B3LYP is somewhat surprising, and there is no experimental information available on this splitting to compare with. Previous theoretical results for this singlet triplet splitting are 4.6 kcal/mol obtained from the MR-SDCI-CASSCF calculations in ref 18, 15.0 kcal/mol obtained from the DFT calculations in ref 34, and 17.3 kcal/mol obtained in ref 33. The Rh–C distance is 1.80 Å for the singlet state and 1.90 Å for the triplet. The singlet state has a clear d^8 character, with two d-electrons contributing to the metal–carbon double bond. The triplet state has considerable character of d^7s mixed in (0.33 s, 7.82 d), which is needed in order to form the double bond. For the triplet state, the metal contributes with one s and one d electron to the double bond. The sd overlap is poor on the metal, which results in a longer metal–carbon distance for the triplet compared to the singlet.

As can be seen from Table 1 and the Figure 1, the potential surfaces calculated at the B3LYP and PCI-80 levels are quite parallel. For the singlet surface there is a rather constant shift of about 7 kcal/mol between the two methods, with the PCI-80 results lower in energy; i.e., the PCI-80 method gives somewhat stronger Rh–C and Rh–H bonds than the B3LYP method for this state. For the triplet surface on the other hand, the B3LYP method gives the lowest energy, in particular during the later steps of the H_2 elimination reaction, where the shift between the two surfaces is about 5 kcal/mol. The main conclusion from the results obtained in the present study is that the PCI-80 and the B3LYP results agree fairly well. However, the fact that the potential surfaces for the two spin states are shifted in opposite directions leads to the rather large difference in the RhCH_2^+ singlet–triplet splitting calculated by the two methods, as mentioned above.

Experimental information is available for two other reaction paths following the C–H insertion, H atom elimination, leaving $\text{RhCH}_3^+ + \text{H}$ as end products, and CH_3 elimination, leaving $\text{RhH}^+ + \text{CH}_3$. The reaction $\text{Rh}^+ + \text{CH}_4 \rightarrow \text{RhCH}_3^+ + \text{H}$ is endothermic by 69.4 kcal/mol according to experiment.¹⁶ The B3LYP energy, 66.1 kcal/mol, is in good agreement with experiment. It turns out that the PCI-80 method overestimates the correlation effect in the Rh–C bond (see below), yielding an endothermicity of only 57.6 kcal/mol. The alternative reaction path, $\text{Rh}^+ + \text{CH}_4 \rightarrow \text{RhH}^+ + \text{CH}_3$, is endothermic by 65.0 kcal/mol according to experiment.¹⁶ B3LYP gives an endothermicity of 58.1 kcal/mol, in somewhat better agreement with experiment than the PCI-80 result of only 55.9 kcal/mol.

As mentioned in the preceding paragraph the PCI-80 method overestimates the Rh–R binding energy in RhH^+ and RhCH_4^+ , while the RhCH_2^+ binding energy is in good agreement with experiment. To investigate the source of this problem, the correlation effects on the binding energy of a series of MH^+ , MCH_2^+ , and MCH_3^+ systems were calculated. In Figure 3 the variation of the correlation effect in the M–R bond energy is shown for a number of second-row metals. The binding

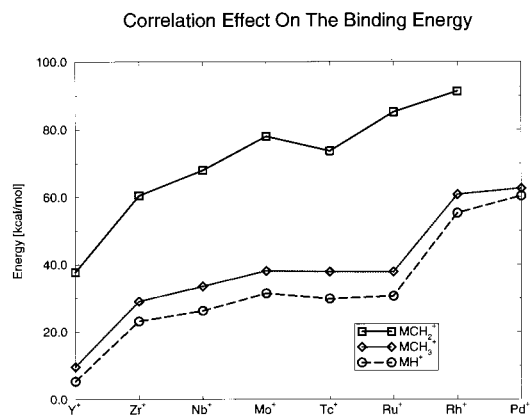


Figure 3. Correlation effect on the binding energy for second-row metal complexes (relative to the s^1 state on the metal ion).

energies are calculated relative to the s^1 state on the metal ion for all the metals. The correlation effect becomes larger when going from left to right in the periodic table, owing to the increasing number of d electrons. Also, the correlation effects in the MCH_2^+ complexes are larger than in MCH_3^+ and MH^+ owing to the metal–carbon double bond. Both these effects are expected. For the correlation effects on the MH^+ and MCH_3^+ complexes, there is a sudden jump in the increase of the correlation effects in going from Ru to Rh and Pd. This can be taken as an indication that MCPF, and hence PCI-80, overestimates the correlation effects in the RhH^+ , RhCH_3^+ , PdH^+ and PdCH_3^+ systems. Actually, also the binding energies in PdH^+ and PdCH_3^+ are found to be considerably larger than experimental values, while for the rest of the second-row transition metals reasonable agreement with available experimental results is obtained.³⁵ In most cases this kind of breakdown of the MCPF method can be detected from large coefficients in the configuration expansion. In a few cases, including RhH^+ and RhCH_3^+ , however, there are no particularly large coefficients, and the reason for this is that a configuration mixing of valence bond type is present between states that require very different orbitals. Since a common set of orbitals is used for these states in the calculations, the effects are spread out among a large number of configurations and no single large coefficient stands out. A similar situation occurred for the Ni atom in a recent study of C–H activation in methane by naked first-row transition metal atoms.³⁶

4. Conclusions

For the reaction $\text{Rh}^+ + \text{CH}_4 \rightarrow \text{RhCH}_2^+ + \text{H}_2$, the experimental value¹⁶ for the endothermicity is 22.6 kcal/mol. The theoretical value obtained in the present study is 20.5 kcal/mol at the PCI-80 level and 28.0 kcal/mol at the B3LYP level. Both the singlet and triplet surfaces for the H_2 elimination reaction have been studied, and the results of the two methods agree well with each other. On the triplet potential surface there is a high barrier, 11.6 kcal/mol (PCI-80) or 13.8 kcal/mol (B3LYP) above the endothermicity of the reaction, corresponding to a multicenter transition state leading directly from the C–H insertion product to the $\text{Rh}(\text{CH}_2)(\text{H}_2)^+$ molecular complex. On the singlet potential surface, which is the ground state after the C–H insertion product has been passed, there is no barrier in excess of the endothermicity, neither at the PCI-80 nor at the B3LYP level, in agreement with the experimental information. In this case the reaction goes via a H- α elimination step leading to the $\text{Rh}(\text{CH}_2)\text{H}_2^+$ dihydride.

For the alternative reaction paths $\text{Rh}^+ + \text{CH}_4 \rightarrow \text{RhH}^+ + \text{CH}_3$ and $\text{Rh}^+ + \text{CH}_4 \rightarrow \text{RhCH}_3^+ + \text{H}$, the B3LYP results agree fairly well with experiment. The experimental endothermicity¹⁶ for the reaction $\text{Rh}^+ + \text{CH}_4 \rightarrow \text{RhH}^+ + \text{CH}_3$ is 65.0 kcal/mol, and the B3LYP calculations give a value of 58.1 kcal/mol. For the reaction $\text{Rh}^+ + \text{CH}_4 \rightarrow \text{RhCH}_3^+ + \text{H}$, the experimental endothermicity¹⁶ is 69.4 kcal/mol, and the B3LYP calculations give 66.1 kcal/mol. For these two reaction products, RhCH_3^+ and RhH^+ , the MCPDF method, and thus also PCI-80, is found to exaggerate the correlation effects, yielding too large Rh–R bond energies. This problem with the PCI-80 is quite unusual but has occurred in a few other cases, e.g. in the NiHCH₃ system.³⁶

References and Notes

- (1) Janowicz, A. H.; Bergman, R. G. *J. Am. Chem. Soc.* **1982**, *104*, 352.
- (2) Janowicz, A. H.; Bergman, R. G. *J. Am. Chem. Soc.* **1983**, *105*, 3929.
- (3) Jones, W. D.; Fehler, F. J. *J. Am. Chem. Soc.* **1982**, *104*, 4240.
- (4) Hoyano, J. K.; Graham, W. A. G. *J. Am. Chem. Soc.* **1982**, *104*, 3723.
- (5) Hoyano, J. K.; McMaster, A. D.; Graham, W. A. G. *J. Am. Chem. Soc.* **1983**, *105*, 7190.
- (6) Armentrout, P. B.; Kickel, B. L. In *Organometallic Ion Chemistry*; Kluwer: Dordrecht, 1995.
- (7) Eller, K.; Schwarz, H. *Chem. Rev.* **1991**, *91*, 1121–1177.
- (8) Irikura, K. K.; Beauchamp, J. L. *J. Phys. Chem.* **1991**, *95*, 8344.
- (9) Musaev, D. G.; Morokuma, K. *Isr. J. Chem.* **1993**, *33*, 307.
- (10) Blomberg, M. R. A.; Siegbahn, P. E. M.; Svensson, M. *J. Phys. Chem.* **1994**, *98*, 2062.
- (11) Heinemann, C.; Wesendrup, R.; Schwarz, H. *Chem. Phys. Lett.* **1995**, *239*, 75.
- (12) Pavlov, M.; Blomberg, M. R. A.; Siegbahn, P. E. M.; Wesendrup, R.; Heinemann, C.; Schwarz, H. *J. Phys. Chem. A* **1997**, *101*, 1567.
- (13) Byrd, G. D.; Freiser, B. S. *J. Am. Chem. Soc.* **1982**, *104*, 5944.
- (14) Tolbert, M. A.; Mandich, M. L.; Halle, L. F.; Beauchamp, J. L. *J. Am. Chem. Soc.* **1986**, *108*, 5675.
- (15) Jacobson, D. B.; Freiser, B. S. *J. Am. Chem. Soc.* **1985**, *107*, 5870.
- (16) Chen, Y.; Armentrout, P. B. *J. Phys. Chem.* **1995**, *99*, 10775.
- (17) Albert, G.; Berg, C.; Beyer, M.; Achatz, U.; Joos, S.; Niedner-Schatteburg, G.; Bondybey, V. E. *Chem. Phys. Lett.* **1997**, *268*, 235.
- (18) Musaev, D. G.; Koga, N.; Morokuma, K. *J. Phys. Chem.* **1993**, *97*, 4064.
- (19) Becke, A. D. *Phys. Rev. A* **1988**, *38*, 3098.
- (20) Becke, A. D. *J. Chem. Phys.* **1993**, *98*, 1372.
- (21) Becke, A. D. *J. Chem. Phys.* **1993**, *98*, 5648.
- (22) Stevens, P. J.; Devlin, F. J.; Chabrowski, C. F. *J. Phys. Chem.* **1994**, *98*, 11623.
- (23) Siegbahn, P. E. M.; Blomberg, M. R. A.; Svensson, M. *Chem. Phys. Lett.* **1994**, *223*, 35–45.
- (24) Siegbahn, P. E. M.; Svensson, M.; Boussard, P. J. E. *J. Chem. Phys.* **1995**, *102*, 5377–5386.
- (25) Chong, D. P.; Langhoff, S. R. *J. Chem. Phys.* **1986**, *84*, 5606.
- (26) Pople, J. A.; Head-Gordon, M.; Fox, D. J.; Raghavachari, K.; Curtiss, L. A. *J. Chem. Phys.* **1989**, *90*, 5622.
- (27) STOCKHOLM is general purpose quantum chemical set of programs, written by Per E. M. Siegbahn, Margareta R. A. Blomberg, Lars G. M. Pettersson, Björn O. Roos, and Jan Almlöf.
- (28) Hay, P. J.; Wadt, W. R. *J. Chem. Phys.* **1985**, *82*, 299.
- (29) Huzinaga, S. *J. Chem. Phys.* **1977**, *66*, 4245.
- (30) Blomberg, M. R. A.; Siegbahn, P. E. M.; Svensson, M. *J. Chem. Phys.* **1996**, *104*, 9546.
- (31) Blomberg, M. R. A.; Siegbahn, P. E. M.; Svensson, M. *New J. Chem.* **1991**, *15*, 727.
- (32) Ziegahn, P. E. M.; Svensson, M. *J. Am. Chem. Soc.* **1994**, *116*, 10124.
- (33) Perry, J. K. Ph.D. thesis, Caltech, 1994.
- (34) Russo, N. In *Metal ligand interaction: from atoms to clusters to surfaces*; Kluwer: Dordrecht, 1992.
- (35) Blomberg, M. R. A. To be published.
- (36) Wittborn, A. M. C.; Costas, M.; Blomberg, M. R. A.; Siegbahn, P. E. M. *J. Chem. Phys.* **1997**, *107*, 4318.